Copy No. _____

Defence Research and Development Canada
Recherche et développement pour la défense Canada

DEFENCE R&D DÉFENSE

RANS calculations of the flow past inclined propellers

Paul-Edouard Leras
ENSIETA, Brest, France

David Hally
DRDC Atlantic

Defence R&D Canada – Atlantic

Technical Memorandum
DRDC Atlantic TM 2009-266
May 2010

Canada

This page intentionally left blank.

RANS calculations of the flow past inclined propellers

Paul-Edouard Leras
ENSIETA, Brest, France

David Hally
DRDC Atlantic

Defence R&D Canada – Atlantic

Technical Memorandum

DRDC Atlantic TM 2009-266

May 2010

Principal Author

Original signed by David Hally

David Hally

Approved by

Original signed by D. Hopkin

D. Hopkin
Head/Maritime Asset Protection

Approved for release by

Original signed by R. Kuwahara for

C. Hyatt
Chair/Document Review Panel

Abstract

The flow code ANSYS CFX has been used to calculate the flow around two model propellers, DTMB P4679 and DTMB P4718, operating with a 7.5° shaft inclination. Pressures on the face and back of the blades have been compared with measured values. The predictions agree well with measured average pressures and in the amplitude of the variations in pressure. Predictions of the phase of the pressure variations are not as good. The ANSYS CFX predictions also compare favourably with the predictions of panel methods, especially with regard to the amplitude of the pressure variations.

Résumé

Le code d'écoulement ANSYS CFX a été utilisé pour calculer l'écoulement autour de deux modèles d'hélices, DTMB P4679 et DTMB P4718, fonctionnant selon une inclinaison des arbres porte-hélices de 7,5°. Les pressions exercées sur l'avant et l'arrière des pales ont été comparées aux données mesurées. Les prédictions concordent bien avec les pressions moyennes mesurées et avec l'amplitude de variation de la pression. Cependant, les prédictions de la phase de variation de la pression ne sont pas aussi bonnes. Les prédictions d'ANSYS CFX concordent aussi avec les prédictions effectuées avec un groupe témoin, tout spécialement en matière d'amplitude de variation de la pression.

This page intentionally left blank.

Executive summary

RANS calculations of the flow past inclined propellers

Paul-Edouard Leras, David Hally; DRDC Atlantic TM 2009-266; Defence R&D Canada – Atlantic; May 2010.

Background: The Maritime Asset Protection Section at DRDC Atlantic is using Reynolds-averaged Navier-Stokes (RANS) solvers to predict the flow around propellers so that the noise generated by propeller cavitation can be predicted. The current document reports calculations to validate that unsteady pressures on propeller blades can be predicted accurately.

Principal results: The RANS solver ANSYS CFX (ANSYS, Inc.) was used to calculate the flow around two model propellers, DTMB P4679 and DTMB P4718, operating with a 7.5° shaft inclination to induce unsteady inflow. Pressures on the face and back of the propeller were compared with measurements as well as with calculations reported by other researchers using panel methods. ANSYS CFX predictions agree well with measured average pressures and in the amplitude of the variations in pressure. Predictions of the phase of the pressure variations are not as good. The ANSYS CFX predictions also compare favourably with the predictions of panel methods, especially with regard to the amplitude of the pressure variations.

Significance of results: These calculations are evidence that ANSYS CFX will be able to predict unsteady flow over propellers accurately and so will be a useful tool for predicting cavitation and resulting radiated noise from ships.

Future work: Further validation needs to be done, in particular using non-uniform inflows and propellers for which accurate measurements of the propeller vortices are available. Then the emphasis will shift to predicting cavitation within the propeller vortices and developing radiated noise models.

Sommaire

RANS calculations of the flow past inclined propellers

Paul-Edouard Leras, David Hally ; DRDC Atlantic TM 2009-266 ; R & D pour la défense Canada – Atlantique ; mai 2010.

Introduction : La division de la Protection des biens maritimes de RDDC Atlantique utilise les solutionneurs de l'Analyse d'équations Navier-Stokes moyennées (RANS) pour prédire l'écoulement autour des hélices et le niveau de bruit engendré par la cavitation des hélices. Le document actuel comprend des calculs qui attestent qu'il est possible de prédire de façon précise les pressions instables exercées sur les pales d'hélices.

Résultats : Le solutionneur RANS ANSYS CFX (ANSYS, Inc.) a été utilisé pour calculer l'écoulement autour de deux modèles d'hélices, DTMB P4679 et DTMB P4718, fonctionnant selon une inclinaison des arbres porte-hélices de 7,5°, laquelle permet de créer un débit entrant instable. Les pressions exercées sur l'avant et l'arrière de l'hélice ont été comparées avec les données de même qu'avec les calculs signalés par d'autres chercheurs utilisant des méthodes avec groupe témoin. Les prédictions de l'ANSYS CFX concordent avec les pressions moyennes mesurées et avec l'amplitude de variation de la pression. Cependant, les prédictions de la phase de variation de la pression ne sont pas aussi bonnes. Les prédictions d'ANSYS CFX concordent aussi avec les prédictions effectuées avec un groupe témoin, tout spécialement en matière de l'amplitude de variation de la pression.

Portée : Ces calculs démontrent que l'ANSYS CFX sera en mesure de prédire de façon précise l'écoulement instable sur les hélices. Il constituera donc un outil utile pour prédire la cavitation et l'émission de bruit des navires.

Recherches futures : Une validation ultérieure doit être effectuée, tout spécialement avec des hélices pour lesquelles des données précises en matière de tourbillon fixe à l'intérieur de débits entrants non homogènes sont disponibles. L'accent sera ensuite placé sur la prédiction de la cavitation à l'intérieur des débits entrants de l'hélice et sur l'élaboration de modèles d'émission de bruit.

Table of contents

List of figures

List of tables

This page intentionally left blank.

1 Introduction

At DRDC Atlantic, panel methods have been used to calculate unsteady flows around propellers for many years. However, panel methods are unable to give good predictions when viscous flow becomes important: e.g. predictions of pressures in tip, leading edge and hub vortices; and predictions of propeller performance at off-design conditions when separation may be important. To address these issues viscous flow solvers must be used. To that end, DRDC Atlantic is investigating the use of Reynolds-averaged Navier-Stokes (RANS) solvers for predicting the flows past propellers. The current study is a preliminary validation exercise to ensure that the RANS solver ANSYS CFX [1] is capable of predicting blade pressures accurately when the inflow is unsteady.

The flows past two propellers, DTMB P4679 and DTMB P4718, were calculated. Each propeller was inclined by 7.5° to the incident flow, thus generating an inflow whose axial component is uniform but whose tangential component rotates as seen in a coordinate system fixed to the propeller. The blade loading is increased when a blade moves in a direction opposite to the tangential inflow, and decreased half a turn later when it moves in the same direction as the tangential inflow.

After brief descriptions of the method of representing the propeller geometry (Section 2) and the method of generating computational grids (Section 3), details of the calculations are described and comparisons made with the experiments of Jessup [2] (Sections 4 and 5). Implications of these results on the ability of ANSYS CFX to make accurate predictions of propeller flows are discuused in Section 6.

2 Propeller geometry

The geometry of each propeller blade is determined by specifying sections from the hub to the tip of a reference blade. Each section is specified by its shape (usually given as a series of offsets from the chord line joining the leading and trailing edges), chord length, pitch, skew angle and total rake. These data are splined to generate a surface representation of the whole blade.

The blade surface generated in this way has a coordinate singularity at the tip which can cause difficulties when creating a grid for the flow calculations. To remove the coordinate singularity the blade surface is split into five separate surfaces:

1. a surface on the lower portion of the blade which wraps around the trailing edge;
2. a surface in the lower middle of the pressure side of the blade;
3. a surface on the lower portion of the blade which wraps around the leading edge;
4. a surface in the lower middle of the suction side of the blade; and

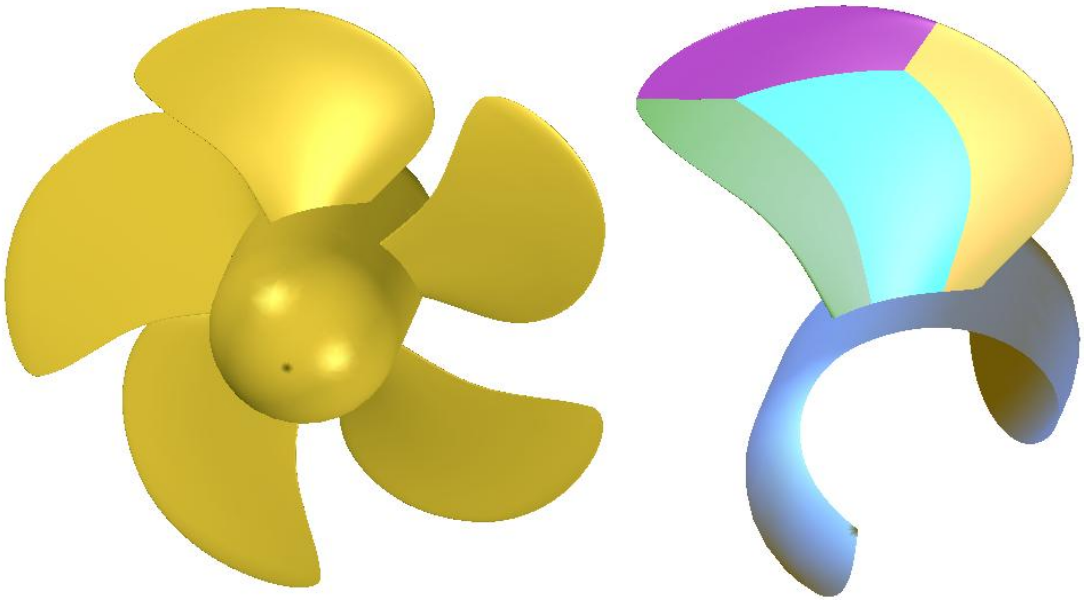

Figure 1: *The full propeller (left) and the portion saved in the IGES file (right). Four of the five blade surfaces can be seen. The fifth is in the centre of the other side of the blade.*

5. a surface on the upper portion of the blade which wraps around both leading and trailing edges.

The last surface is usually smoothed a little near the tip to remove very small radii of curvature caused by the definition in terms of sections.

The hub is an axisymmetric surface specified by a curve which is rotated about the propeller axis. When no data for the actual hub are available, a cylindrical hub with hemispherical end caps is used. The hub is split into sectors, one for each blade. The edge of each sector runs roughly parallel to the line on the hub joining the leading and trailing edges of its blade, tracing a helical shape as it extends to the ends of the hub. The intersection of the hub and the reference blade is calculated and the hub sectors are trimmed by removing the footprints of the blades. The blades are also trimmed so that only the portion above the hub is retained.

The propeller geometry is saved in a file in IGES format [3]. Only the five surfaces on the reference blade, its associated hub sector and the intersection line between the blade and hub are saved. The other blades and the full hub are easily regenerated by copying and rotating the saved portions. Figure 1 shows a propeller along with the decomposition of the blade and hub surface as saved in the IGES file.

3 Gridding strategy

Grids for the flow calculations were generated using the program Pointwise [4] and its scripting language Glyph. The following steps were used:

1. The geometry of the propeller was read from the IGES file.
2. Structured domains (two-dimensional grids) were made on each of the five blade surfaces then smoothed to minimize adverse effects of skewness.
3. The domains on the blades were extruded normal to the blade surfaces to generate an inflation layer for the boundary layers on the blades. The domain edges at the hub were required to follow the hub surface during the extrusion.
4. An unstructured domain was generated on the sector of the hub associated with the blade (the portion of the hub stored in the IGES file: see Figure 1).
5. The hub domain and the blocks on the blades were copied and rotated so that the full hub and all propeller blades were covered.
6. An inflation layer for the hub boundary layer was generated by normal extrusion of the unstructured hub domains. The edges of the extruded block were required to match the lower portions of the blade blocks.
7. A cylindrical shell enclosing the propeller was generated and covered with structured blocks created by normal extrusion from the boundaries. These blocks are only one cell thick.
8. The space between the blocks on the outer cylindrical shell and the blocks on the blades and hub was filled with an unstructured block of pyramid and tetrahedral elements.

An example of the domains on the surface of DTMB P4718 is shown in Figure 2; they are considerably coarser than the grid that was actually used in the RANS calculations. The grid on the surrounding cylindrical shell is shown in Figure 3.

Because all blocks meeting boundaries are created by normal extrusion, each cell on a boundary is oriented very nearly perpendicularly to that boundary. This allows ANSYS CFX to generate an accurate implementation of the boundary conditions.

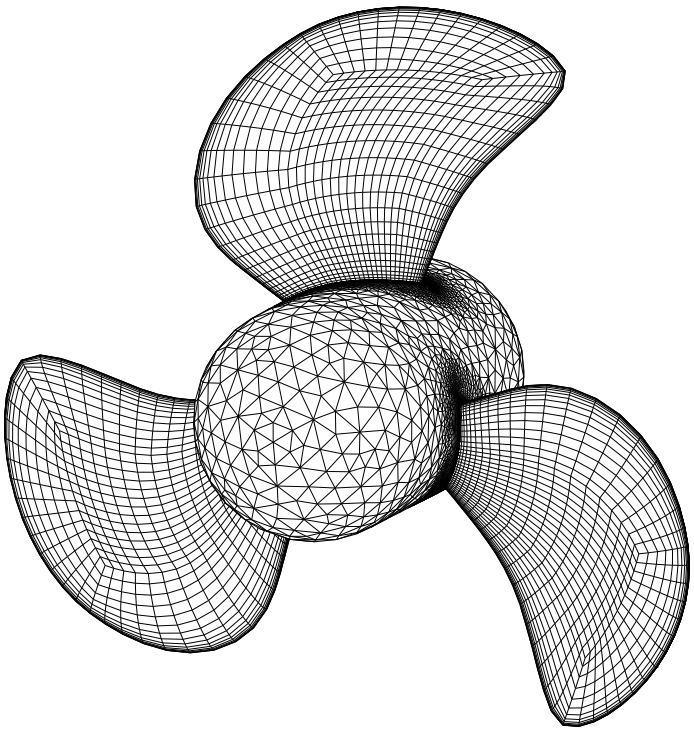

Figure 2: *The grid on the surfaces of the blades and hub of DTMB P4718. This grid is coarser than those used in the calculations.*

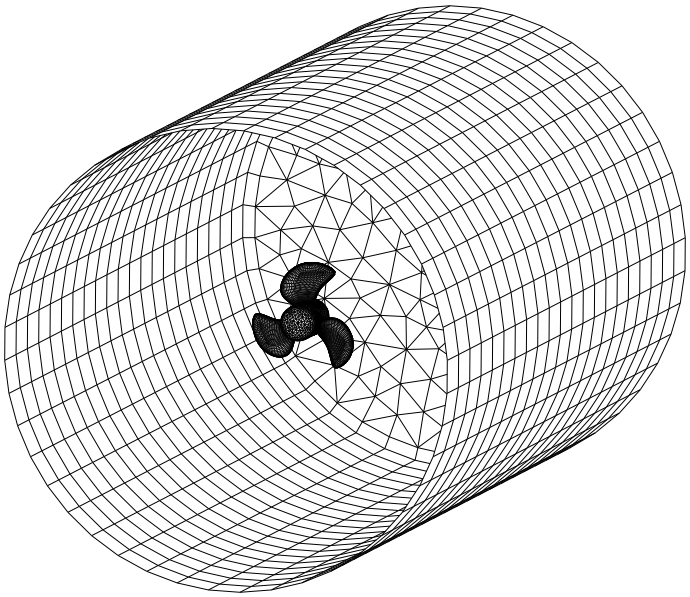

Figure 3: *The grid on the propeller and the outer shell. The grid on the inflow boundary has been removed.*

4 Propeller DTMB P4679

The propeller DTMB P4679 is a three-bladed propeller designed for testing in the David Taylor Model Basin (DTMB) at the Naval Surface Warfare Center, Carderock Division. It has the features of a controllable pitch propeller with a wide chord, high skew and sections based on the DTMB modifications to the NACA 66 airfoil [5]. The wide chords were used to generate a similar loading to a typical five-bladed propeller used by the US Navy; the resulting increase in blade thickness made it easier to embed pressure transducers. Its principal characteristics are shown in Table 1.

Measurements of the pressure on the blades of DTMB P4679 were made by Jessup [2] with the shaft inclined 7.5°. The inclination of the shaft caused a tangential velocity pointing downward from the top of the propeller disk toward the bottom. The pressure was measured at 40 locations having $r = 0.5R$, $0.7R$ or $0.9R$, where R is the propeller radius. The measured pressures are reported as an average value and an amplitude and phase of the first harmonic of the pressure coefficient:

$$C_p = \overline{C}_p + C_{p1}\cos(\theta - \phi) \tag{1}$$

where θ is the angle of propeller rotation measured from top dead centre in the direction of rotation, $\overline{C}_p$ is the average pressure coefficient, C_{p1} is the amplitude of its first harmonic and ϕ is its phase angle. Jessup reports that the amplitudes of higher harmonics were very small.

DTMB P4679 is a challenge to grid because of the complex geometry at the tip. The cambre of all sections exceeds the blade thickness causing the blade to curl along the leading and trailing edges near the tip. The resulting radii of curvature near the tip are very small. To alleviate the problems that this caused during the gridding, the blade geometry was smoothed near the tip.

Figure 4 shows an example of a near vertical cross-section of the blade passing close to the tip both before and after smoothing. The base of the cross-section is at approximately $r = 0.9R$. The curl can clearly be seen as well as the very small radius of curvature at the tip on the original blade. The curl is also shown in Figure 5.

A different gridding problem arose because the blade emerges from the hub obliquely near the

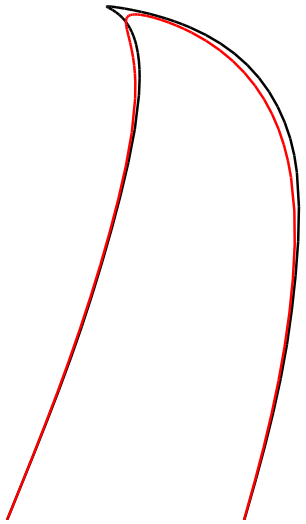

Figure 4: *A near-vertical cross-section through DTMB P4679 passing close to the tip; the original blade in black; the smoothed blade in red.*

Table 1: *Principal characteristics of DTMB P4679*

Diameter, D	0.6096 m
Rotation	Right hand
Number of blades, Z	3
Hub-Diameter ratio	0.3
Expanded Area Ratio	0.755
Design Advance Coefficient, J	1.078
Design Thrust Coefficient, K_T	0.194
Design Torque Coefficient, K_Q	0.0486

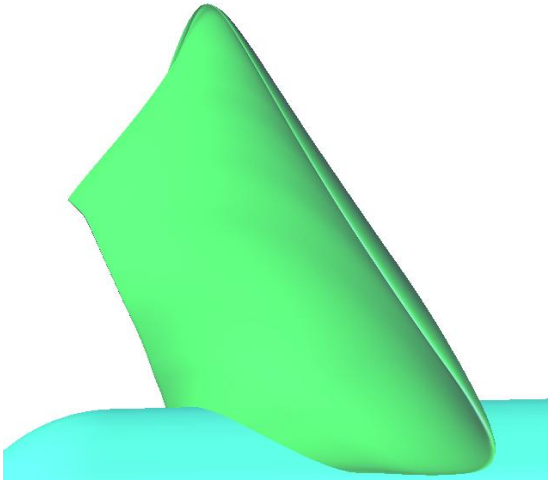

Figure 5: *Propeller DTMB P4679 showing the curl in the blade near the tip.*

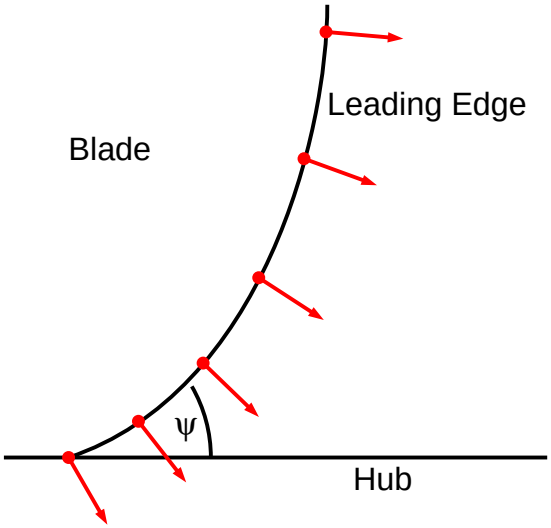

Figure 6: *Extrusion of grid nodes on the leading edge into the hub when the emergence angle, ψ, is small.*

leading edge. Since the extrusion of the blade domains is normal to the blades, an oblique angle of emergence causes the natural location of the extruded nodes to be within the hub: see Figure 6. The smoothing used during the extrusion process will prevent this from happening provided that the extrusion angle is not too far from perpendicular. In the case of DTMB P4679 the smoothing cannot cope and the extrusion fails.

The blade extrusion problem was handled by modifying the blade geometry near the hub so that the blade emerged from it nearly perpendicularly. This was done by reducing the diameter of the hub and adding extra blade sections at $r = 0.25R$ and $r = 0.275R$. The hub itself does not conform to the geometry of the actual propeller: it is simply a cylinder with hemispherical end-caps. The modified geometry is shown in Figure 7 and tabulated in Annex A. The original geometry is given by Jessup [2].

The grid used had 5 million nodes, about three-quarters of which were in the structured

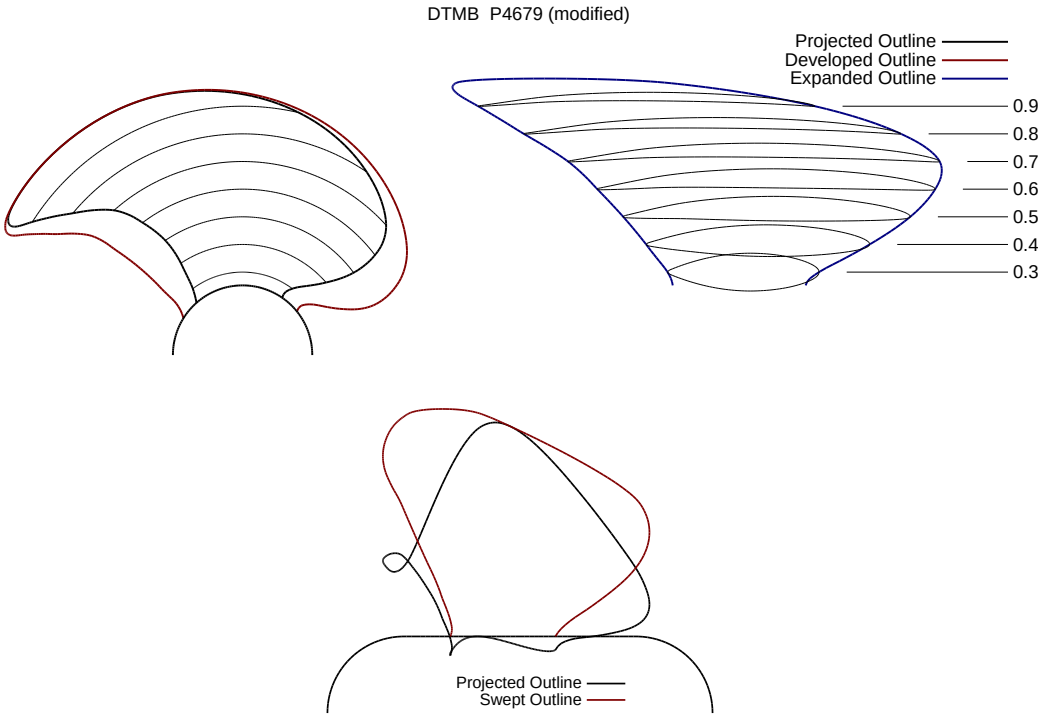

Figure 7: *The modified version of propeller DTMB P4679.*

blocks around the blades. The near wall spacing on the blades was $2 \times 10^{-5} D$ while that on the hub was $5 \times 10^{-5} D$. The resulting y^+ values varied between 4 and 10 over most of the blade with a peak value of 33 near the tip (y^+ is a non-dimensional distance to a solid boundary; it is defined in the list of symbols). The y^+ values varied between 7 and 15 over most of the hub with peak values of 16 near the blade roots. The outer cylindrical shell had radius twice that of the propeller and extended from $1.5R$ upstream of the blade reference line to $2R$ downstream. Larger outer shells have been tried with other propellers — DTMB P4718 in particular: see Section 5 — with very little difference in the predicted values of C_p.

Table 2: *Advance coefficients and corresponding inflow speeds and rotation rates for DTMB P4679.*

J	V	n
1.078	5.39 m/sec	8.20 rps
0.719	3.60 m/sec	8.21 rps

$J = V/nD$ = Advance coefficient;
V = Inflow speed; n = Rotation rate

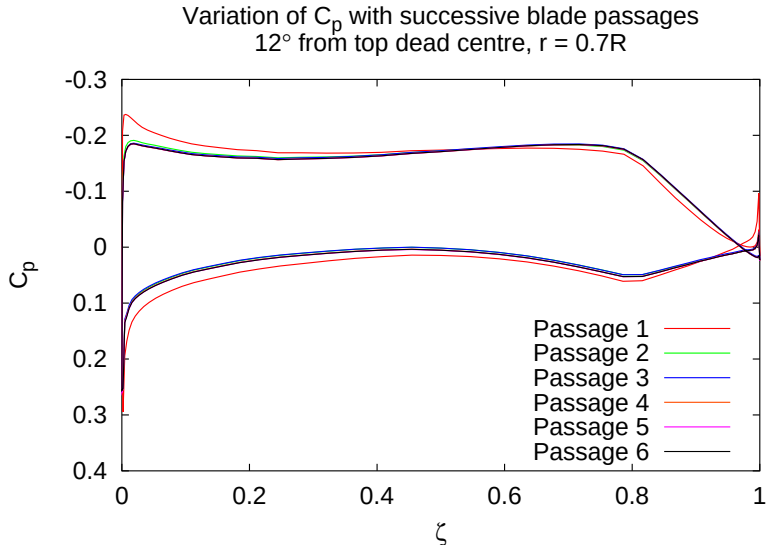

Figure 8: *The variation of C_p with successive blade passages. Each curve represents C_p at $r = 0.7R$ on a single blade as it passes the location 12° past top dead centre in the direction of rotation.*

The flow around P4679 was calculated using ANSYS CFX with the Shear Stress Transport (SST) turbulence model at the design advance coefficient, $J = 1.078$, and at the more highly loaded case, $J = 0.719$. The corresponding inflow velocities and rotation rates are given in Table 2. In each case the simulation lasted for two full rotations of the propeller using a time step equivalent to a three degree rotation: 240 time steps in all. Thirty inner iterations were used per time step. After the first few time steps the RMS momentum residuals levelled out at roughly 2×10^{-4} with maximum residuals near 3×10^{-2}. The momentum residuals were smaller than 10^{-3} everywhere except a small region around the leading edge. The mass residuals were much smaller with RMS values near 10^{-6} and maximum values near 5×10^{-4} near the leading edge. The residuals were slightly larger for the smaller advance coefficient.

After a single blade passage, the non-periodicity due to the initialization had nearly damped out; after two blade passages the flow was nearly perfectly periodic. Figure 8 shows the variation of C_p with successive blade passages on the section with $r = 0.7R$ (the abscissa, ζ, is the fractional chord length from 0 at the leading edge to 1 at the trailing edge). The blade location is fixed at 12° past top dead centre in the direction of rotation. The first blade passage occurs after only four time steps; the pressure on the blade has not yet had time to relax from its initial state ($C_p = 0$ everywhere). However, by the second passage at time step 44 the pressure is very close to its final state. The C_p values at blade passages 3 through 6 are nearly identical.

The calculated mean thrust coefficient, K_T, at the design advance ratio is 0.202 while the

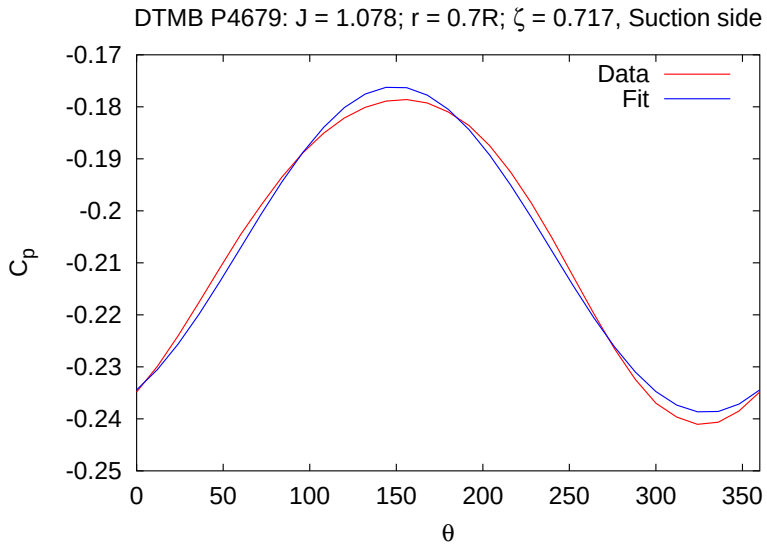

Figure 9: *Comparison of the pressure data at a single point on DTMB P4679 with the fit implied by Equation (1). The abscissae are the angular positions as the point undergoes a full rotation.*

design value quoted by Jessup [2] is 0.194. The calculated mean torque coefficient, K_Q, is 0.0517 while the design value is 0.0486. Jessup does not give measured values.

Pressure values were sampled on each blade at points along the sections at $r = 0.5R$, $0.7R$ and $0.9R$ over the last one-third of a revolution (40 time steps). These data were then combined to generate equivalent pressures on a single blade over a full revolution which were used to determine the values of $\overline{C}_p$, C_{p1} and ϕ.

Figure 9 compares the calculated C_p values at a single point on the blade with the fit to those data obtained using $\overline{C}_p$, C_{p1} and ϕ (see Equation (1)). This point is fairly typical of the fits obtained: some were considerably better, some somewhat worse. The fits right at the leading edge for the design advance coefficient were particularly poor, perhaps influenced by the poor convergence in that region.

Figure 10 compares the measured and calculated values of $\overline{C}_p$, C_{p1} and ϕ at $r = 0.5R$, $0.7R$ or $0.9R$ at the design advance coefficient $J = 1.078$. The RANS calculations agree well with the measured average values. The RANS average C_p values were almost identical to values calculated in a steady flow with no shaft inclination.

Propeller P4679 was used as a test case in a workshop conducted by the Propulsion Committee of the 22nd International Towing Tank Conference (ITTC) [6]; the results from eleven different unsteady panel methods are reported at $r = 0.7R$. Many of the the methods show roughly similar accuracy for the average C_p to that of ANSYS CFX and none is significantly better.

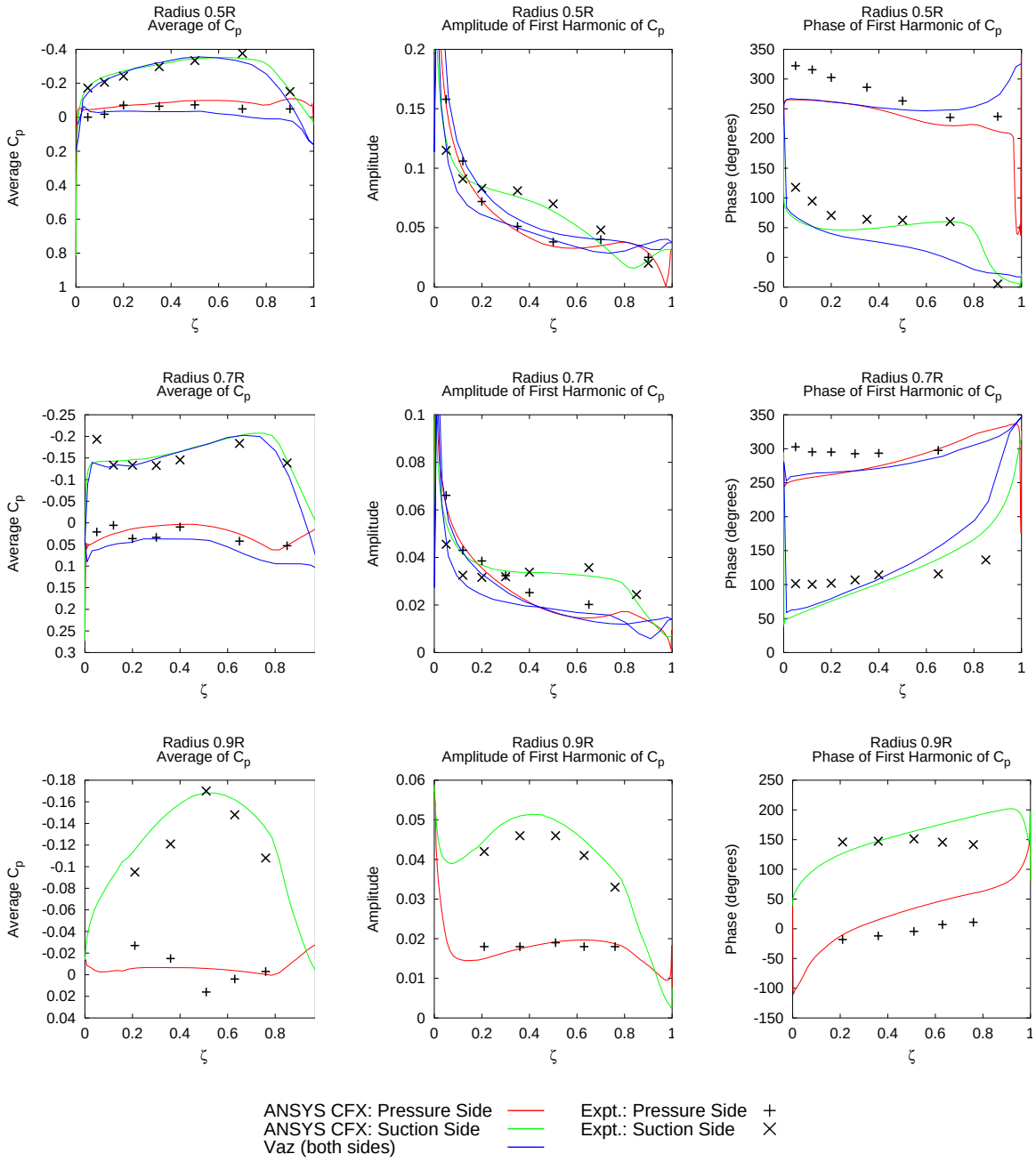

Figure 10: *Measured and calculated averages and amplitudes and phases of the first harmonic of the pressure on DTMB P4679 with* $J = 1.078$. *For* $r = 0.5R$ *and* $0.7R$, *the predictions of Vaz are also shown.*

Calculations on P4679 have also been reported by Vaz [7]. His code forms the basis of the Cooperative Research Ships panel method PROCAL which is also used at DRDC Atlantic. Vaz's results are also shown in Figure 10 for $r = 0.5R$ and $0.7R$; he provides no results for $r = 0.9R$, nor does he discriminate between the pressure and the suction side in his results. The prediction of the average pressure is good but slightly less accurate than the ANSYS CFX results.

It should also be noted that panel methods usually require that the trailing edge closes at a sharp point to ensure that a Kutta condition can be applied and that there will be no problems with flow separation. The ANSYS CFX calculations, on the other hand, used a blunt trailing edge closed using an elliptical cap; the thickness of each section then conforms to the actual propeller geometry except in the immediate vicinity of the trailing edge. These differences may account for differences in predictions very close to the trailing edge.

The ANSYS CFX predictions of the amplitudes of the first harmonics are also very good and are better than all but two of the results reported at the ITTC Propeller Workshop, and worse than none. They are also significantly better than those of Vaz.

Neither ANSYS CFX nor the panel method predict the phase well, though it is interesting to note that the two methods agree on the phase near the leading edge. At $r = 0.5R$ the RANS prediction is significantly better over the pressure side. At $r = 0.7R$ the two predictions are remarkably similar, especially considering the discrepancy with the measured values. Phase results are not reported in Reference 6. A possible source of phase error is when the fit implied by Equation (1) is poor: i.e. when the pressure at a point contains significant higher harmonic content. However, no correlation could be found between poor fits using Equation (1) and poor fits with the experiments. Therefore the presence of higher harmonic content has been ruled out as a source of the phase error.

Figure 11 shows similar calculations for the lower advance coefficient $J = 0.719$. Neither Vaz nor Reference 6 quote results for this case. At $r/R = 0.5$ and 0.7 the agreement with experiment is similar to that at the design advance coefficient. At $r/R = 0.9$, however, the agreement is noticeably worse on the suction side. This may be attributable to cavitation at the tip which is present in the experiments but not accounted for in the calculations.

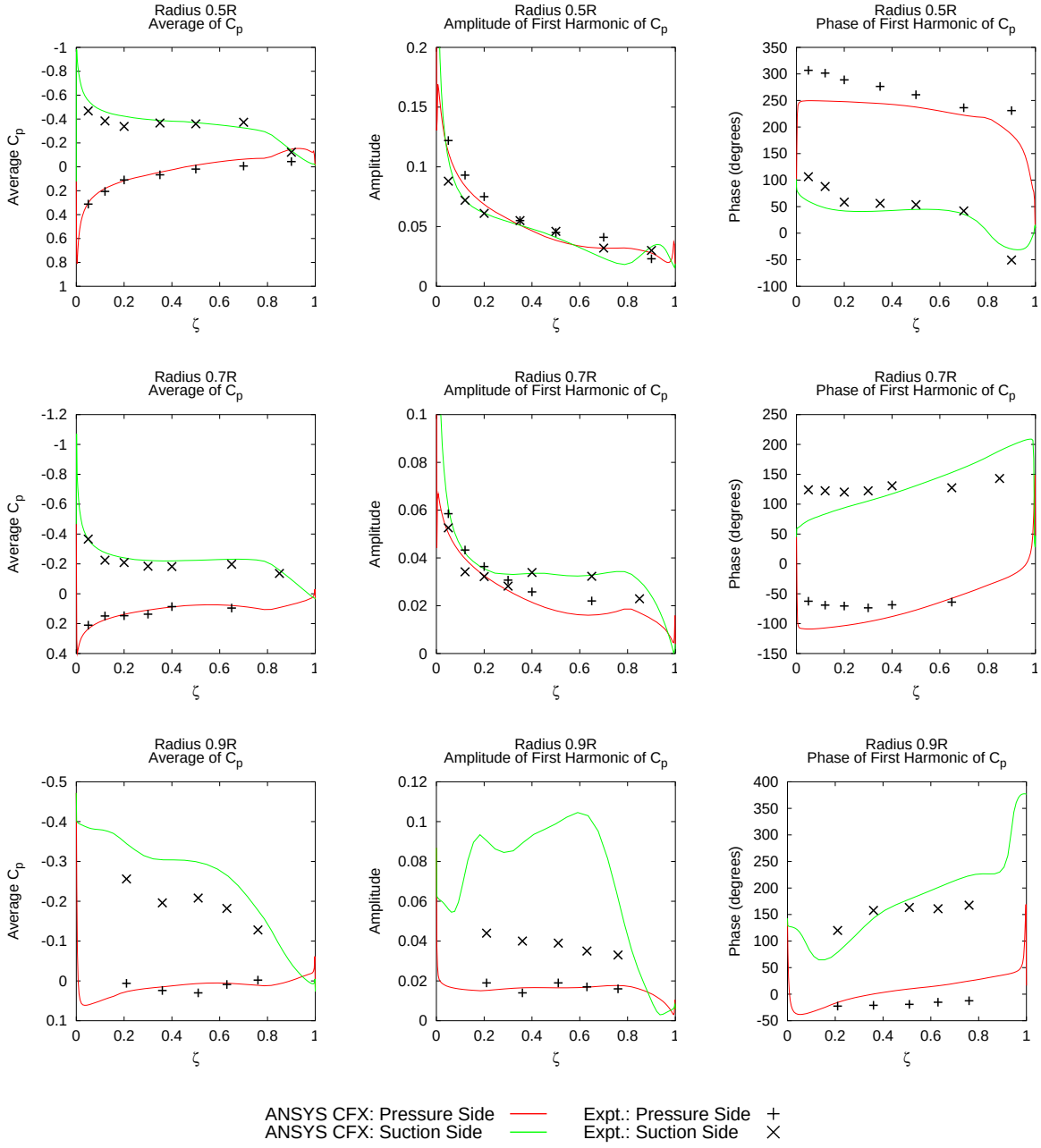

Figure 11: *Measured and calculated averages and amplitudes and phases of the first harmonic of the pressure on DTMB P4679 with* $J = 0.719$.

5 Propeller DTMB P4718

The propeller DTMB P4718 is a three-bladed propeller designed to have similar loading to DTMB P4679 but at a lower design advance coefficient so the propeller would rotate more times during a single run down the towing tank during the experiments. Its skew and width are significantly smaller than DTMB P4679 but, like DTMB P4679, its blade sections are based on the DTMB modifications to the NACA 66 airfoil. Its principal characteristics are shown in Table 3.

As with DTMB P4679, measurements of the pressure on the blades of DTMB P4718 were made by Jessup [2] with the shaft inclined 7.5°. The pressure was measured at 40 locations having $r = 0.5R$, $0.7R$ or $0.9R$.

There were no significant difficulties with gridding DTMB P4718 so the geometry used is as tabulated by Jessup [2] except that the hub was replaced by a simple cylinder of radius $0.3R$ having hemispherical end-caps and extending from $-0.3333D$ upstream of the blade reference line, to $0.3D$ downstream of it. The geometry is shown in Figure 12. The cambre of DTMB P4718 is much smaller than DTMB P4679 so that there are no significant complexities in the geometry of the tip and, due to its smaller width, the blade emerges from the hub at a large enough angle that there were no problems with the extrusion of the blade domains.

The effect of the size of the computational region on the pressure predictions was tested by calculating the steady flow at zero shaft inclination using two different grids, each using the same blocks extruded from the blades and the hub, but differing in the size of the outer shell. The larger grid used an outer shell of radius $4R$ and a length of $6R$ while the smaller had radius $2R$ and length $4R$. The size of the cells near the outer boundaries was kept the same. Figure 13 shows values of C_p at $r = 0.5R$ calculated using the two different grids; the results at other radii are similar. Owing to the small differences, the smaller grid was used for the unsteady calculations.

The grid used had 1.8 million nodes, about three-quarters of which were in the structured

Table 3: *Principal characteristics of DTMB P4718*

Diameter, D	0.6096 m
Rotation	Right hand
Number of blades, Z	3
Hub-Diameter ratio	0.3
Expanded Area Ratio	0.755
Design Advance Coefficient, J	0.751
Design Thrust Coefficient, K_T	0.055
Design Torque Coefficient, K_Q	0.0106

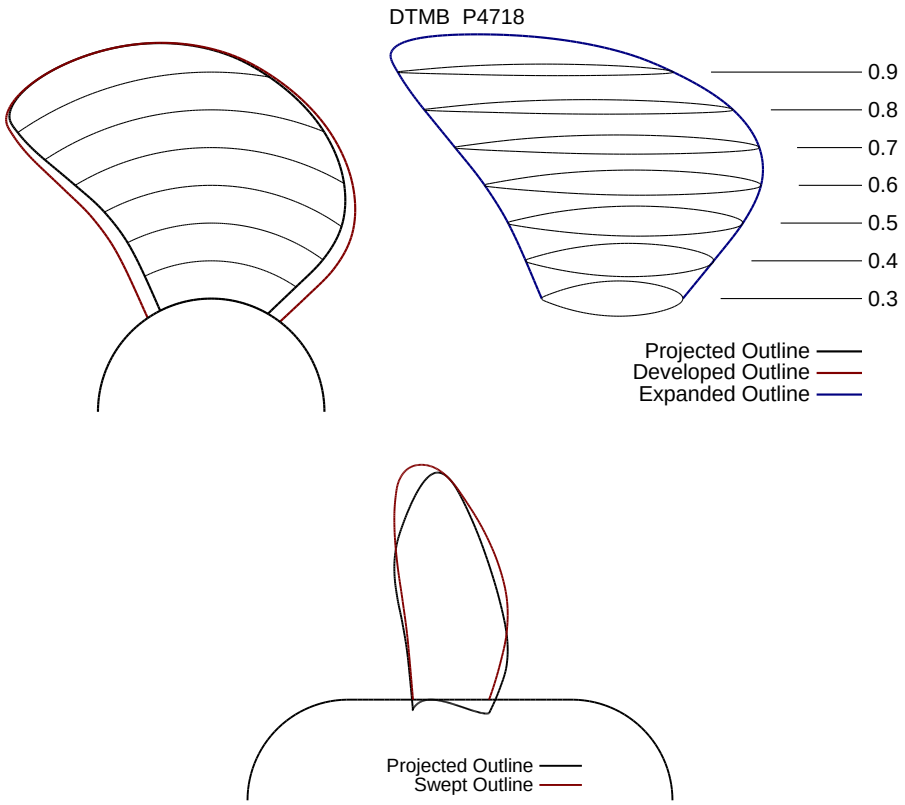

Figure 12: *Propeller DTMB P4718.*

blocks around the blades. The near wall spacing on the blades was $2 \times 10^{-4}D$ while that on the hub was $5 \times 10^{-4}D$. The resulting y^+ values varied between 3 and 100 over the blades. The y^+ values varied between 3 and 100 over most of the hub with peak values of 140 near the blade roots.

The flow around P4718 was calculated using ANSYS CFX with the Shear Stress Transport (SST) turbulence model at the design advance coefficient, $J = 0.751$ ($V = 3.61$ m/sec; $n = 7.88$ rps). In each case the simulation lasted for four full rotations of the propeller using a time step equivalent to a three degree rotation: 480 time steps in all. The RMS residuals were required to be less than 10^{-4}, a level they normally reached after only two inner iterations. The maximum momentum residuals were typically about 10^{-2} located near the upstream end of the hub surface. On the blades the maximum residuals were about 10^{-3} located on the trailing edge near $r = 0.9R$. Other than this region and a small region along the leading edge, the momentum residuals were below 10^{-4} for all nodes close to the blades. The mass residuals were much smaller with RMS values near 10^{-6} and maximum values near 10^{-4} near the trailing edge at $r = 0.9R$.

Pressure values were sampled on each blade at points along the sections at $r = 0.5R$, $0.7R$ and $0.9R$ over the last full revolution (120 time steps). These data were then used to deter-

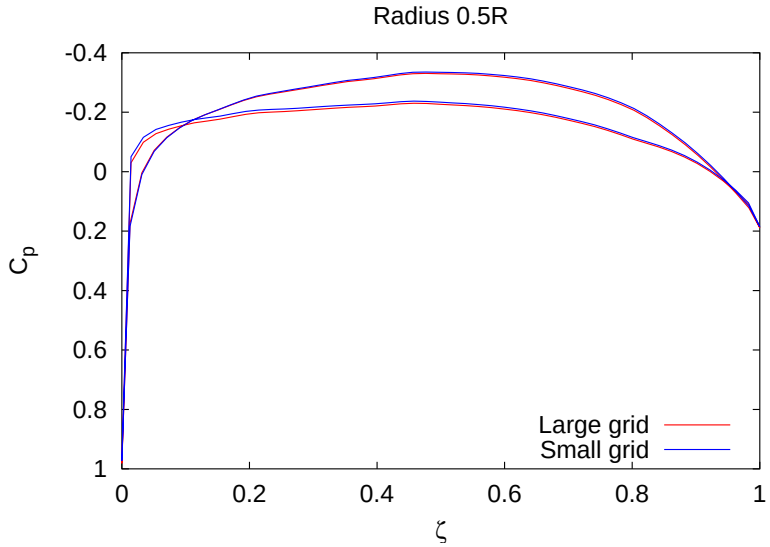

Figure 13: *Values of C_p for DTMB P4718 at $r = 0.5R$ calculated using grids differing in the extent of the flow region.*

mine the values of $\overline{C}_p$, C_{p1} and ϕ.

Figure 14 compares the measured and calculated values of $\overline{C}_p$, C_{p1} and ϕ at $r = 0.5R$, $0.7R$ and $0.9R$. The RANS calculations agree fairly well with the measured average values. It should be noted that the measured values are considered somewhat less accurate than those for DTMB P4679, that being the reason that DTMB P4718 was not chosen as a test case for the ITTC Propeller Workshop. The RANS average C_p values were almost identical to values calculated in a steady flow with no shaft inclination.

Hoshino [8] has reported panel method calculations of the pressures on DTMB P4718 with no shaft inclination; they are of a similar accuracy to those reported here. Unfortunately Hoshino does not consider the unsteady case.

As with DTMB P4679, the predictions of the amplitudes of the first harmonics are very good, the phase predictions less so. However, at $r = 0.5R$ and $r = 0.7R$ on the pressure side, while the phase angles are underpredicted, the sudden drop in phase angle is captured well.

The fits to the data using Equation (1) were roughly of the same quality as those for DTMB P4679 (see Figure 9). At several locations, in particular at $r = 0.7R$ and $r = 0.9R$ on the aft half of the pressure side of the blade, the amplitude of the pressure variation, C_{p1}, is very small resulting in degraded quality of fit (for example, see Figure 15). One should expect poorer phase predictions in these locations; however, the reasons for poor phase predictions elsewhere are unknown.

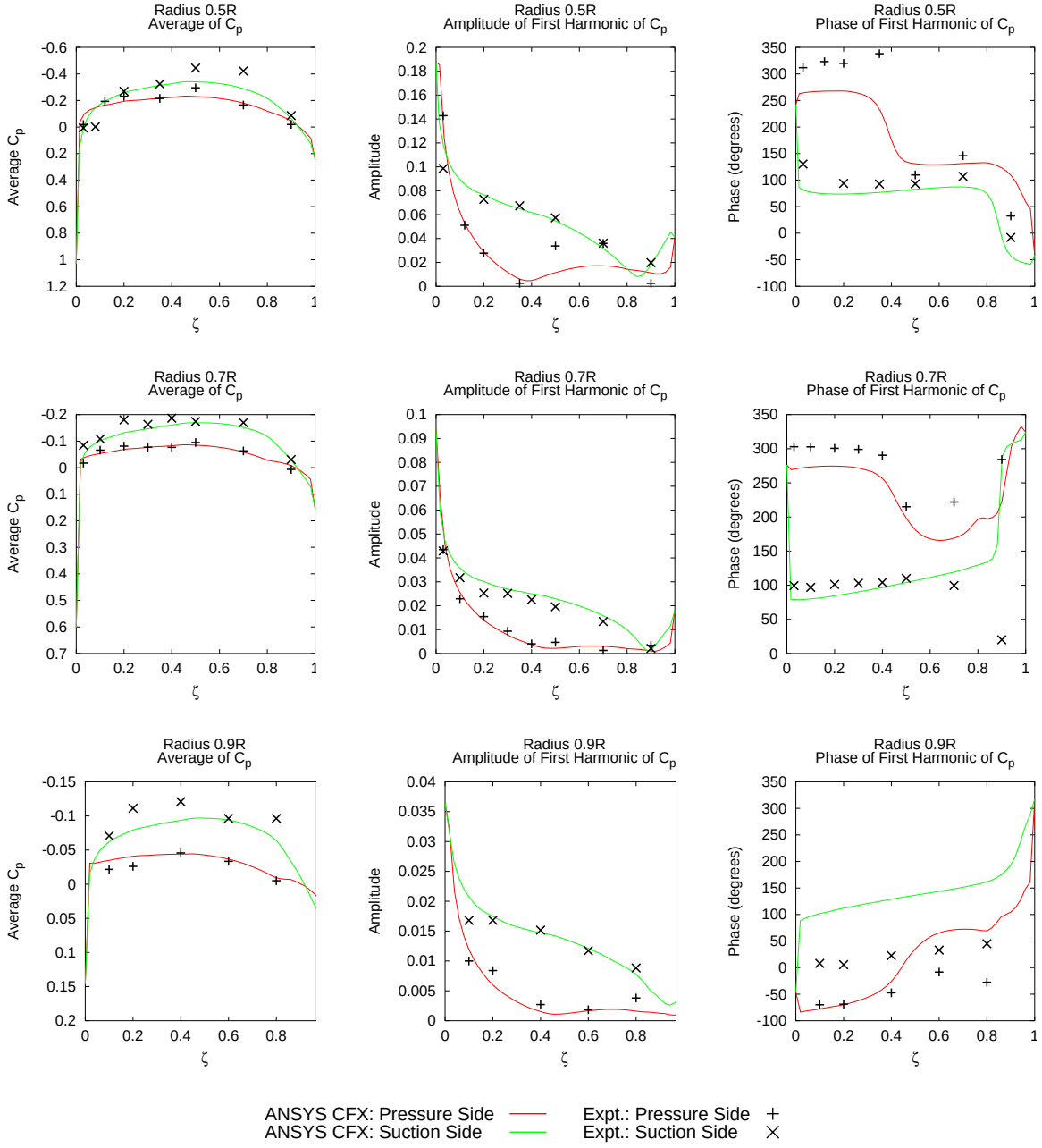

Figure 14: *Measured and calculated averages and amplitudes and phases of the first harmonic of the pressure on DTMB P4718 with* $J = 1.078$.

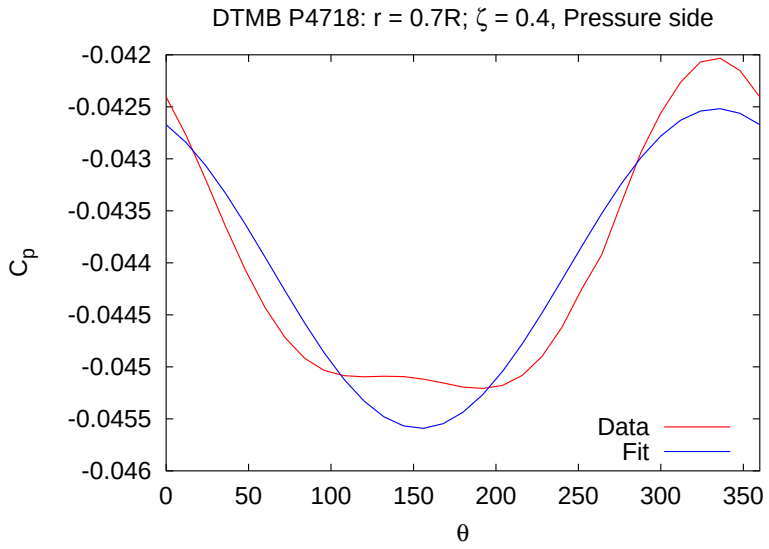

Figure 15: *Comparison of the pressure data at a single point on DTMB P4718 with the fit implied by Equation (1). The abscissae are the angular positions as the point undergoes a full rotation. At this location C_{p1} is very small and the fit is correspondingly poor.*

6 Concluding remarks

The results presented in Sections 4 and 5 are very encouraging, especially considering that these propellers were designed to mimic existing naval propellers. For propeller DTMB P4679, where there are panel method predictions available for comparison, the ANSYS CFX predictions of the average pressure are similar to the predictions of most of the panel methods, but much more accurate than all but two in predictions of the amplitudes of the pressure variation. The accuracy of the predictions for DTMB P4718 are similar in accuracy to those of DTMB P4679.

However, this is the simplest form of unsteady propeller flow; validation of flows with non-uniform inflow will also be necessary. Also, these calculations have not tested the ability of ANSYS CFX to predict the flow within the various propeller vortices accurately, a necessity if it is to be used for predicting vortex cavitation. Further validation is necessary using propellers for which accurate measurements of the vortices are available.

References

[1] (2009), ANSYS CFX (online), ANSYS, Inc., http://www.ansys.com/products/cfx.asp (Access Date: November 2009).

[2] Jessup, S. D. (1982), Measurement of the Pressure Distribution on Two Model Propellers, (Report DTNSRDC-82/035) David W. Taylor Naval Ship Research and Development Center.

[3] (1988), Initial Graphics Exchange Specification (IGES) Version 4.0, US Dept. of Commerce, National Bureau of Standards. Document No. NBSIR 88-3813.

[4] (2009), Pointwise: Reliable CFD Meshing You Trust (online), Pointwise, Inc., Fort Worth, Texas, http://www.pointwise.com (Access Date: November 2009).

[5] Brockett, T. (1966), Minimum Pressure Envelopes for Modified NACA-66 Sections with NACA a = 0.8 Camber and BuShips Type I and Type II Sections, (Report 1780) David W. Taylor Naval Ship Research and Development Center.

[6] (1999), The Propulsion Committee: Final Report and Recomendations to the 22nd ITTC. Available on-line at http://ittc.sname.org/Propulsion.pdf. (Access Date: November 2009).

[7] Vaz, G. N. V. B. (2005), Modelling of Sheet Cavitation on Hydrofoils and Marine Propellers using Boundary Element Methods, Ph.D. thesis, Universidade Técnica de Lisboa, Instituto Superior Técnico, Lisbon, Portugal.

[8] Hoshino, T. (1991), Numerical and Experimental Analysis of Propeller Wake by Using a Surface Panel Method and a 3-Component LDV, In *Proceedings of the Eighteenth Symposium on Naval Hydrodynamics*, pp. 297–313, National Academies Press.

Annex A: Modified geometry of DTMB P4679

Table A.1 defines the geometry of the modified version of DTMB P4679. Each section uses the DTMB modification of the NACA 66 airfoil as defined by Brockett [5]. The hub is a circular cylinder of radius $0.252R$ having hemispherical end-caps; it extends from $-0.3333D$ upstream of the blade reference line, to $0.3D$ downstream of it.

The lowest two sections have been added to make the blade emerge from the hub at nearly right angles.

Table A.1: *Section characteristics of the modified DTMB P4679*

r/R	t/c	F/c	P/D	c/D	Ψ (deg.)	I_t/D
0.250	0.3115	0.0000	0.812	0.240	3.44	0.012
0.275	0.2806	0.0000	0.881	0.250	2.29	0.006
0.300	0.2496	0.0000	0.950	0.274	0.00	0.000
0.350	0.1877	0.0090	1.088	0.340	-4.52	-0.014
0.375	0.1630	0.0132	1.157	0.373	-6.22	-0.020
0.400	0.1418	0.0171	1.225	0.404	-7.56	-0.026
0.450	0.1088	0.0238	1.349	0.464	-9.25	-0.035
0.500	0.0855	0.0287	1.449	0.519	-9.73	-0.039
0.550	0.0690	0.0313	1.516	0.568	-9.18	-0.039
0.600	0.0566	0.0321	1.556	0.611	-7.94	-0.035
0.650	0.0462	0.0316	1.576	0.646	-6.18	-0.027
0.700	0.0378	0.0306	1.572	0.672	-3.14	-0.014
0.750	0.0318	0.0298	1.537	0.685	1.83	0.008
0.800	0.0281	0.0293	1.475	0.682	8.00	0.033
0.850	0.0262	0.0289	1.388	0.658	14.62	0.057
0.900	0.0254	0.0287	1.270	0.609	22.28	0.079
0.950	0.0249	0.0287	1.120	0.518	31.48	0.098
0.975	0.0248	0.0283	1.041	0.431	36.36	0.105
0.990	0.0248	0.0279	0.995	0.335	39.27	0.109
1.000	0.0248	0.0274	0.965	0.000	41.18	0.111

t = max. section thickness; F = max. section cambre; P = pitch;
c = chord length; Ψ = skew angle; I_t = total rake

List of symbols

θ The angle of propeller rotation measured from top dead centre of the reference blade in the direction of propeller rotation.

ϕ Phase angle of the first harmonic of the pressure coefficient.

Ψ Skew angle.

ψ Emergence angle of the blade leading edge from the hub.

ζ Fractional chord length along a blade section: $\zeta = 0$ at the leading edge, 1 at the trailing edge.

c Chord length of a blade section.

C_p Pressure coefficient.

$\overline{C}_p$ Average pressure coefficient.

C_{p1} Amplitude of the first harmonic of the pressure coefficient.

D Propeller diameter.

F Maximum cambre of a blade section.

J Advance coefficient.

K_T Thrust coefficient.

K_Q Torque coefficient.

n Rotation rate.

I_t Total rake.

r Radial coordinate equal to the distance from the propeller axis.

P Pitch.

R Propeller radius.

t Maximum thickness of a blade section.

V Inflow speed.

y^+ Non-dimensional distance to a solid boundary;

$$y^+ = \frac{y}{\nu}\sqrt{\frac{\tau}{\rho}}$$

where y is the distance to the wall, ν is the kinematic viscosity, ρ is the fluid density and τ is the shear stress.

Z Number of blades.

This page intentionally left blank.

Distribution list

DRDC Atlantic TM 2009-266

Internal distribution

1 Principal Author

3 Library (1 paper, 2 CDs)

Total internal copies: 4

External distribution

Department of National Defence

1 DRDKIM

2 DMSS 2

Others

1 Library and Archives Canada
395 Wellington Street
Ottawa, Ontario
K1A ON4
Attn: Military Archivist, Government Records Branch

1 Director-General
Institute for Ocean Technology
National Research Council of Canada
P.O. Box 12093, Station A
St. John’s, Newfoundland
A1B 3T5

1 Director-General
Institute for Aerospace Research
National Research Council of Canada
Building M-13A
Ottawa, Ontario
K1A OR6

1 Transport Development Centre
Transport Canada
6th Floor
800 Rene Levesque Blvd, West
Montreal, Que.
H3B 1X9
Attn: Marine R&D Coordinator

MOUs

6 Canadian Project Officer ABCA-02-01 (C/SCI, DRDC Atlantic – 3 paper copies, 3 PDF files on CDROM)

Total external copies: 13

Total copies: 17

DOCUMENT CONTROL DATA

(Security classification of title, body of abstract and indexing annotation must be entered when document is classified)

1. ORIGINATOR (The name and address of the organization preparing the document. Organizations for whom the document was prepared, e.g. Centre sponsoring a contractor's report, or tasking agency, are entered in section 8.)

   Defence R&D Canada – Atlantic
   PO Box 1012, Dartmouth NS B2Y 3Z7, Canada

2. SECURITY CLASSIFICATION (Overall security classification of the document including special warning terms if applicable.)

   UNCLASSIFIED

3. TITLE (The complete document title as indicated on the title page. Its classification should be indicated by the appropriate abbreviation (S, C or U) in parentheses after the title.)

   RANS calculations of the flow past inclined propellers

4. AUTHORS (Last name, followed by initials – ranks, titles, etc. not to be used.)

   Leras, P.-E.; Hally, D.

5. DATE OF PUBLICATION (Month and year of publication of document.)

   May 2010

6a. NO. OF PAGES (Total containing information. Include Annexes, Appendices, etc.)

   36

6b. NO. OF REFS (Total cited in document.)

   8

7. DESCRIPTIVE NOTES (The category of the document, e.g. technical report, technical note or memorandum. If appropriate, enter the type of report, e.g. interim, progress, summary, annual or final. Give the inclusive dates when a specific reporting period is covered.)

   Technical Memorandum

8. SPONSORING ACTIVITY (The name of the department project office or laboratory sponsoring the research and development – include address.)

   Defence R&D Canada – Atlantic
   PO Box 1012, Dartmouth NS B2Y 3Z7, Canada

9a. PROJECT OR GRANT NO. (If appropriate, the applicable research and development project or grant number under which the document was written. Please specify whether project or grant.)

   Project 11cw04

9b. CONTRACT NO. (If appropriate, the applicable number under which the document was written.)

10a. ORIGINATOR'S DOCUMENT NUMBER (The official document number by which the document is identified by the originating activity. This number must be unique to this document.)

   DRDC Atlantic TM 2009-266

10b. OTHER DOCUMENT NO(s). (Any other numbers which may be assigned this document either by the originator or by the sponsor.)

11. DOCUMENT AVAILABILITY (Any limitations on further dissemination of the document, other than those imposed by security classification.)

   (X) Unlimited distribution
   ( ) Defence departments and defence contractors; further distribution only as approved
   ( ) Defence departments and Canadian defence contractors; further distribution only as approved
   ( ) Government departments and agencies; further distribution only as approved
   ( ) Defence departments; further distribution only as approved
   ( ) Other (please specify):

12. DOCUMENT ANNOUNCEMENT (Any limitation to the bibliographic announcement of this document. This will normally correspond to the Document Availability (11). However, where further distribution (beyond the audience specified in (11)) is possible, a wider announcement audience may be selected.)

13. ABSTRACT (A brief and factual summary of the document. It may also appear elsewhere in the body of the document itself. It is highly desirable that the abstract of classified documents be unclassified. Each paragraph of the abstract shall begin with an indication of the security classification of the information in the paragraph (unless the document itself is unclassified) represented as (S), (C), or (U). It is not necessary to include here abstracts in both official languages unless the text is bilingual.)

The flow code ANSYS CFX has been used to calculate the flow around two model propellers, DTMB P4679 and DTMB P4718, operating with a 7.5° shaft inclination. Pressures on the face and back of the blades have been compared with measured values. The predictions agree well with measured average pressures and in the amplitude of the variations in pressure. Predictions of the phase of the pressure variations are not as good. The ANSYS CFX predictions also compare favourably with the predictions of panel methods, especially with regard to the amplitude of the pressure variations.

14. KEYWORDS, DESCRIPTORS or IDENTIFIERS (Technically meaningful terms or short phrases that characterize a document and could be helpful in cataloguing the document. They should be selected so that no security classification is required. Identifiers, such as equipment model designation, trade name, military project code name, geographic location may also be included. If possible keywords should be selected from a published thesaurus. e.g. Thesaurus of Engineering and Scientific Terms (TEST) and that thesaurus identified. If it is not possible to select indexing terms which are Unclassified, the classification of each should be indicated as with the title.)

Computational fluid dynamics
Fluid flow
Propellers
ANSYS CFX
Pointwise
Pointwise Glyph

This page intentionally left blank.

Defence R&D Canada

Canada's leader in defence
and National Security
Science and Technology

R & D pour la défense Canada

Chef de file au Canada en matière
de science et de technologie pour
la défense et la sécurité nationale

www.drdc-rddc.gc.ca